Coexistence of the Meissner and Vortex States on a Nanoscale Superconducting Spherical Shell

Co-existence of the Meissner and Vortex-state on a superconducting spherical shell

J. Tempere[1,2*], V.N. Gladilin[1,3], I.F. Silvera[2], J.T. Devreese[1] and V.V. Moshchalkov[3]

[1]*TFVS, Universiteit Antwerpen, Groenenborgerlaan 171, B-2020 Antwerpen, Belgium.*

[2]*Lyman Laboratory of Physics, Harvard University, Cambridge MA02318, USA.*

[3]*INPAC, Katholieke Universiteit Leuven, Celestijnenlaan 200D, B-3001 Leuven, Belgium.*

* jacques.tempere@ua.ac.be

Vortices are ubiquitous in charge and matter flows, appearing in diverse systems ranging from nanosuperconductors to planets and neutron stars. Controlling and understanding vortex behavior and creating a guided vortex (fluxon) motion in superconductors is crucial for developing new fluxonics devices [1-5]. Whereas much effort has gone into mastering vortex dynamics in a layer of superconductor through nanopatterning of flat surfaces, the possibilities offered by engineering the geometry and topology of such surfaces have not yet been fully exploited. Here we show that on superconducting surfaces curved into spherical nanoshells the Meissner state can co-exist with a variety of unusual vortex patterns. This co-existence aids superconductivity and drives the phase transition to higher magnetic fields. The spherical geometry leads to a Magnus-Lorentz force driving the nucleating vortices and antivortices towards the poles, overcoming local pinning centers, preventing vortex-antivortex recombination and leading to a Meissner belt around the sphere's equator.

Several key experiments have demonstrated how different vortex patterns can be created and guided in mesoscopic and nanoscopic superconductors [1-4]. These

breakthroughs in the pursuit of 'fluxonics' have focused on hybrid superconductor/ferromagnet nanosystems [1-2], or on the use of nanostructured superconductors [3-4]. Here, we investigate how the geometry (curvature and topology) of the superconducting layer rather than the patterning can be used to control flux. In particular, we focus on spherical nanoshells. These are nanoparticles consisting of a dielectric core of typically 50-200 nm in radius, coated by a 5-20 nm thin metallic shell [6].

In the Ginzburg-Landau formalism, superconductors are described by a macroscopic wave function $\psi=|\psi|e^{i\varphi}$ that couples to the electromagnetic field and that takes the role of the order parameter for the superconducting phase. The interpretation of this wave function is straightforward: its modulus square $|\psi|^2$ corresponds to the density of Cooper pairs, whereas the gradient of its phase φ relates to the supercurrent.

We focus on superconducting nanoshells with a shell thickness substantially smaller than both the London penetration depth λ_L (that also defines the radius of maximum circular supercurrent) and the correlation length ξ (that also defines the vortex core size). This requirement simplifies the treatment in two important ways. First, the external magnetic field will be only weakly perturbed by the nanoshell. Second, the order parameter will be constant in the shell along the radial direction, so ψ will only depend on the spherical angles $\Omega=\{\theta,\phi\}$. Confining ψ to the shell leads to an effective κ that differs from its bulk value, where $\kappa_{bulk}=\lambda_L/\xi$.

Bulk superconductors expel the magnetic field and form a Meissner state up to a critical field strength H_{c1}. When exposed to larger fields, type II superconductors allow the magnetic field to penetrate in the form of quantized superconducting vortices, up to a field H_{c2} above which the superconductivity is fully suppressed. Superconducting

nanoshells exhibit a very similar behavior (with adapted values of the critical field), as can be easily seen from a variational argument.

Consider the following experiment. We prepare the system with a vortex along the z-axis, at a magnetic field $H_{c1}<H<H_{c2}$. Then we ramp down the magnetic field to a value $H<H_{c1}$ where the Meissner state has a lower free energy than the vortex state. How will the vortex initially prepared vanish from the system? The initial state consists of a vortex line threading the spherical shell through the poles, and with vorticity pointing to the 'north' pole ($\theta=0$). The superflow is confined to the shell. The vortex line punctures the shell in two points, forming 'cores' around which the two-dimensional superflow on the surface takes place. The two-dimensional (2D) superflow on the northern hemisphere ($\theta<\pi/2$) rotates anticlockwise around the unit vector $\mathbf{e}_r$ at the core, whereas on the southern hemisphere ($\theta>\pi/2$) it rotates clockwise around the unit vector $\mathbf{e}_r$ at the southern core. We will refer to the local flow pattern on the northern hemisphere as a 2D-vortex and to that on the southern hemisphere as a 2D-antivortex. When the vortex line, still parallel to the north-south axis, is moved away from the poles (so as to expel vorticity from the system), the 2D vortex and 2D antivortex move on their respective hemispheres towards the equator. There, they can merge, and the clockwise and anticlockwise flows cancel each other out, leaving a uniform order parameter.

When the dynamics described above is calculated in the framework of the Ginzburg-Landau equations and using a variational ansatz, we find that the external magnetic field gives rise to an energy barrier (shown in Fig. 1) that pushes the 2D vortex and the 2D antivortex away from the equator and towards the poles, separating the pair. This is in remarkable contrast with flat superconducting films, where vortex-antivortex pairs tend to annihilate.

What is the origin of the trapping potential pushing the vortices towards the poles? The presence of even a weak magnetic field acts like an additional flow with velocity field $H\sin(\theta)$ rotating the superfluid, as shown in the inset of Fig. 1. Around the core of the vortex there is a circular superflow, so that on one side of the vortex, the magnetic field contribution to the superfluid adds up to the vortex superflow, and on the other side it subtracts. If the magnetic field and the vorticity vector point to the same hemisphere (north or south), the resulting Magnus-Lorentz force will push the 2D-vortex towards the poles. When multiple single vortices are present, they aggregate at the poles, forming a vortex lattice region.

Expressing the Ginzburg-Landau equations in hydrodynamic form, the resulting equations for superfluid velocity and Cooper pair density are formally equivalent to the shallow-atmosphere Euler equations used to model atmospheric dynamics [7]. The role of pressure is taken by the sum of the chemical potential and the quantum pressure, and the viscosity is set to zero. The rotation of the earth drags the atmosphere and provides a flow like the magnetic field flow contribution in the superconducting nanoshells. As a result, there is a surprising correspondence between the behavior of atmospheric vortices (cyclones) on the macroscopic globe and superconducting vortices on the nanoshell. This is illustrated in Fig. 2 for the vortex migration from the equator to the poles, and in Fig. 3. for the formation of polar vortex lattices.

The equatorial region remains a vortex-free ‘Meissner state’, although a shielding current is present. The remarkable co-existence, on the same superconducting film surface, of both a vortex state and the Meissner state is a result of topology, absent in flat thin films. The Meissner belt at the equator represents a Cooper pair reservoir tangent to the magnetic field. In the context of granular superconductors, it was shown by de Gennes that connecting a wire that is unaffected by the magnetic field, to a loop where vorticity is present, aids the superconductivity in the loop [8]. In the case of a

nanoshell, we find that the co-existence of the Meissner belt with the vortex lattice at the poles aids superconductivity in a similar way: in Fig. 4 we compare the nanoshell superconductivity phase diagram to that of disks, and find that the vortex region is enhanced: superconducting nanoshells tolerate larger magnetic fields than superconducting disks.

Vortices can only be expelled, or nucleated, near the equator, where the metastability energy barrier is high, enabling flux hysteresis. In Fig. 5, the full black curves show the Gibbs free energy of the ground state as a function of the magnetic field, for a given shell geometry. The ground state (black curve) is labeled by the integer L, the number of quanta of vorticity present. When the magnetic field is switched on, it needs to be ramped up (following the green, dashed line) to a value of $H \approx 4.15 >> H_{c1}$ before vorticity enters the sphere. As the magnetic field is lowered, vorticity is gradually expelled (following the red dotted curve in Fig. 5). However, the state without a vortex is only reached for $H \approx -0.05$. This means that the vortex remains in the nanoshell even though the magnetic field is switched off completely: a small negative field is required to expel the flux. Flux hysteresis is clearly present, also for other nanoshell sizes. We emphasize that here the flux is trapped not by flux pinning at imperfections, but rather by the topology of the system itself.

The particular dynamics of vortices entering the shell is revealed by the time-dependent Ginzburg-Landau equations, and shown in Fig. 5 (a)-(d). Our numerical results demonstrate that the distribution of supercurrents, typical for a pair of 2D vortices, appears only when the separation between the vortex cores is of the order of the twice the coherence length. As a consequence, vortex cores can only be present outside a Meissner belt of latitudes $\pm\Delta\theta_M \approx \arctan[R/(2\xi)]$ around the equator. Note that mapping this result on the Earth's atmosphere with ξ=150 km gives the a hurricane-free

Meissner belt of 3° latitude around the equator, in agreement with the terrestrial cyclone distributions shown in Fig. 2.

In nanoscopic superconductors, confinement potentials and periodic modulation of material parameters have been explored as tools to manipulate flux and quantum coherence. These advances have made possible the development of e.g. flux transistors, lenses, and switches. Here, we have shown that also the geometry of the sample can be used to manipulate flux. The spherical shell geometry leads to two properties radically different from that of flat superconducting films: first, 2D-vortex-antivortex pairs tend to separate rather than annihilate, and second the curvature enables the co-existence of a vortex state and a Meissner (non-vortex) belt close to the equator on the same surface. These properties aid superconductivity in the device and lead to a strong hysteresis effect with respect to the applied magnetic field is demonstrated, paving the way for a 'flux memory'. Flux storage and guiding is a major goal in the development of fluxonic devices, and superconducting nanoshells are revealed here to be very relevant to reach this goal.

Method

We apply the Ginzburg-Landau formalism to the shell geometry, and obtain the following result for the Gibbs free energy difference between the superconducting state and the normal state (in the same external magnetic field):

$$\Delta G = \int d\Omega \left\{ \left(\nabla_\Omega \psi\right)^2 + |\psi|^2 \left[\nabla_\Omega \varphi - H \sin(\theta)\mathbf{e}_\phi\right]^2 - 2R^2|\psi|^2\left(1 - \frac{1}{2}|\psi|^2\right)\right\}. \quad (1)$$

In this expression, we use spherical coordinates with the z-axis parallel to the magnetic field such that $\nabla_\Omega = \mathbf{e}_\theta(\partial/\partial\theta) + [\mathbf{e}_\phi/\sin(\theta)](\partial/\partial\phi)$. Two experimentally tunable parameters remain: the ratio R of the shell radius $\mathcal{R}$ to $\sqrt{2}$ times the coherence length, and the magnetic field, entering the equation through H, the number of elementary flux quanta

$\Phi_0=h/(2e)$ piercing the equatorial plane of the sphere – here h is Planck's constant and e is the electron charge. The Gibbs free energy is expressed in units $\Phi_0^2/(\sqrt{2}\lambda_L\mu)$ with μ the permeability of the shell material.

In our numerical treatment of superconducting states on spherical nanoshells, we exploit the time-dependent Ginzburg-Landau equations following from (1). These are known to be a powerful tool for studying both the dynamic and the static properties of vortices in nanoscopic and mesoscopic superconductors. For the thin nanoshells under consideration, the behavior of the order parameter is governed by

$$\frac{\partial\psi}{\partial\tau} = \left[\nabla_\Omega - iH\sin(\theta)\mathbf{e}_\phi\right]^2\psi + 2R^2\psi\left(1-|\psi|^2\right) \qquad (2)$$

where the dimensionless variable τ is linked to the time t by the relation $\tau=Dt/\mathcal{R}^2$ with D the normal-state diffusion constant. The finite-difference scheme, applied to solve Eq. (2), is similar to that of Ref. [9], with necessary adaptations to the case of the spherical two-dimensional system. Two-dimensional grids used in our calculations typically have ≥100 equally spaced nodes in the θ-interval from 0 to π, and ≥150 nodes on the ϕ-interval from 0 to 2π. Cyclic boundary conditions are applied at ϕ=0 and ϕ=2π. The boundary conditions at θ=0 and θ=π are determined by the requirement that ψ at the poles becomes constant and independent of ϕ. The time step τ is automatically adapted in the course of the calculation. This adaptation is aimed to minimize the number of steps in τ necessary to approach a steady solution of Eq. (2) and – at the same time – to keep the solving procedure convergent. On average, the step in τ is ~10^{-5} to ~10^{-4} depending on the grid used as well as on R and H. When starting at τ = 0 from a random distribution of ψ (with $|\psi|<<1$), a (meta)stable solution of Eq. (2) is achieved typically at $\tau \le 100$.

While the above simulations are performed for idealized spherically symmetric nanoshells, in realistic nanoshells, inevitable imperfections may perturb the trapping

potential for vortices, just as the presence of continents or mountainous archipelagos perturb atmospheric vortices. In order to model the effect of those imperfections, we have considered nanoshells with spatial variations of the Ginzburg-Landau parameter κ. According to the results of our calculations, though inhomogeneity of κ usually tends to destabilize metastable vortex states, this destabilizing effect on vortex trapping is not dramatic in the case of relatively small variations of κ. Our results imply that vortex trapping should be robust also with respect to moderate deviations of the nanoshell shape from sphericity.

1. Martin, J.I., Velez, M., Nogues, J. & Schuller, I.K. Flux Pinning in a Superconductor by an Array of Submicrometer Magnetic Dots. *Phys. Rev. Lett.* **79**, 1929 (1997).

2. Lange, M., Van Bael, M. J., Bruynseraede, Y. & Moshchalkov V.V., Nanoengineered Magnetic-Field-Induced Superconductivity. *Phys. Rev. Lett.* **90**, 197006 (2003).

3. Harada, K., Kamimura, O., Kasai, H., Matsuda, T., Tonomura, A. & Moshchalkov, V. V. Direct Observation of Vortex Dynamics in Superconducting Films with Regular Arrays of Defects. *Science* **274**, 1167 (1996).

4. Moshchalkov, V.V., Gielen, L., Dhallé, M., Van Haesendonck, C. & Bruynseraede, Y. Quantum interference in a mesoscopic superconducting loop. *Nature* **361**, 617 (1993).

5. de Souza Silva C.C., Van de Vondel J., Morelle M. & Moshchalkov V.V., Controlled multiple reversals of a ratchet effect, *Nature* **440**, 651 (2006).

6. Averitt R. D., Sarkar D. & Halas N. J., Plasmon Resonance Shifts of Au-Coated Au_2S Nanoshells: Insight into Multicomponent Nanoparticle Growth, *Phys. Rev. Lett.* **78**, 4217 (1997).

7. D.R. Durran, *Numerical Methods for Wave Equations in Geophysical Fluid Dynamics*, Springer, Berlin, 1999.

8. P.G. De Gennes, *Compes Rendus Acad. Sci., Sér. II*, **292**, 279 (1981).

9. Vickery P. J., Skerlj P. F., Steckley A. C. Twisdale L. A., Hurricane Wind Field model for use in hurricane simulations, *Journ. Struct. Engineering* **126**, 1203 (2000).

Competing financial interests – The authors declare that they have no competing financial interests.

Supplementary Information, such as additional graphs showing the hysteresis effect for different parameters and animations of vortex dynamics on the nanoshell, accompanies the paper on **www.nature.com/nature**.

Acknowledgments – This work was supported in part by the Fund for Scientific Research – Flanders project nos. G.0356.06, G.0115.06, G.0435.03, G.0306.00, the W.O.G. project WO.025.99N, the GOA BOF UA 2000 UA, and the Department of Energy, Grant No. DE-FG02-ER45978. J.T. gratefully acknowledges support of the Special Research Fund of the University of Antwerp, BOF NOI UA 2004. The authors declare no competing interests.

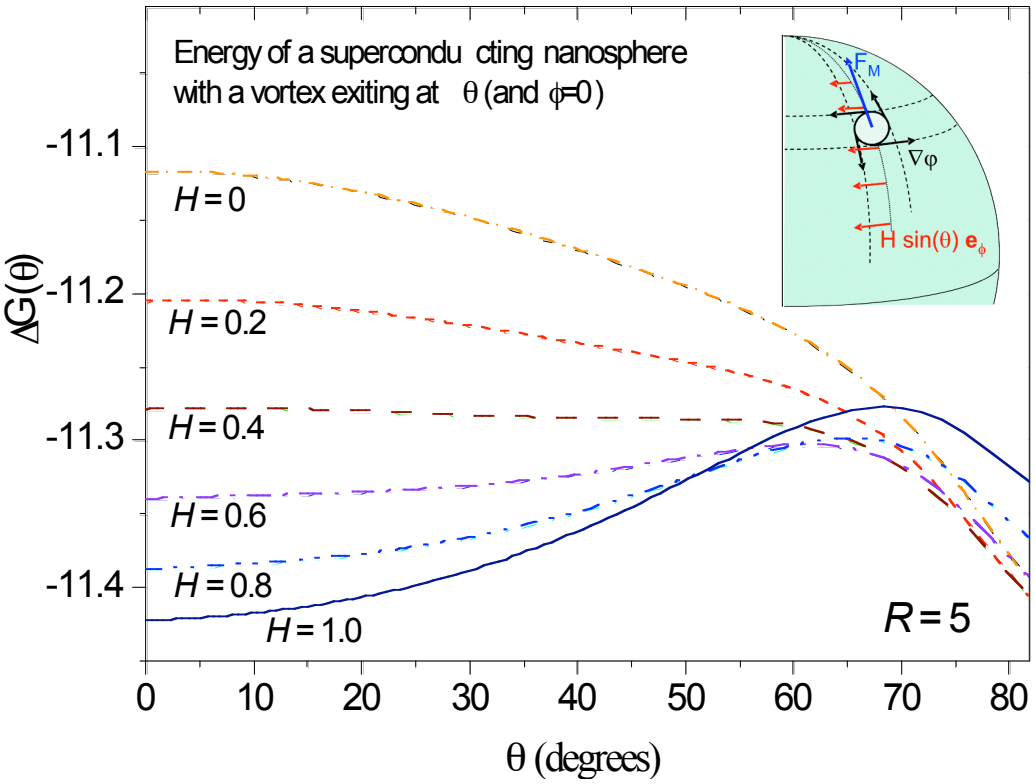

Figure 1 | Gibbs free energy of the vortex state. The Gibbs free energy of a superconducting nanoshell with a vortex line parallel to the *z*-axis and exiting the sphere at an angle θ from the poles, is shown for different values of the magnetic field H as a function of θ. The magnetic field H is expressed in number of elementary flux quanta Φ_0 piercing the equatorial plane. For $H = 0$ the system can lower its energy continuously by shifting the vortex line towards the equator (θ: $0 \rightarrow \pi/2$). The vortex state is unstable, and its 2D-vortex and 2D-antivortex on the shell attract each other, coalesce at the equator, expelling vorticity from the sphere. When H is increased, at $H \approx 0.4$ a plateau in the energy is formed, and for $H > 0.4$ a metastability barrier appears. At $H = 0.6$, the energy of the state without vorticity ($\theta_v = \pi/2$) is lower than the state with a vortex line threading the poles ($\theta_v = 0$), but in order to expel the vortex one has to overcome the energy barrier. There is a trapping potential pushing the vortices to the poles causing the vortex state to be metastable. The vortex will remain metastably trapped if it

is more ‘polar’ (i.e. more north on the northern hemisphere and more south on the southern hemisphere) than a critical latitude. The metastability barrier becomes larger as *H* increases, and the critical latitude shifts closer to the equator. When *H* becomes even larger (than the lower critical field), the energy becomes a continuously increasing function of θ, so that the vortices become stably trapped at the poles. The origin of the metastability barrier is a Magnus-Lorentz F_M force pushing vortices towards the poles, as illustrated in the inset. This force arises from a differential velocity field across the vortex due to the interplay between the supercurrent of the vortex, proportional to the phase gradient $\nabla\varphi$, and the screening supercurrent induced by the magnetic field *H*.

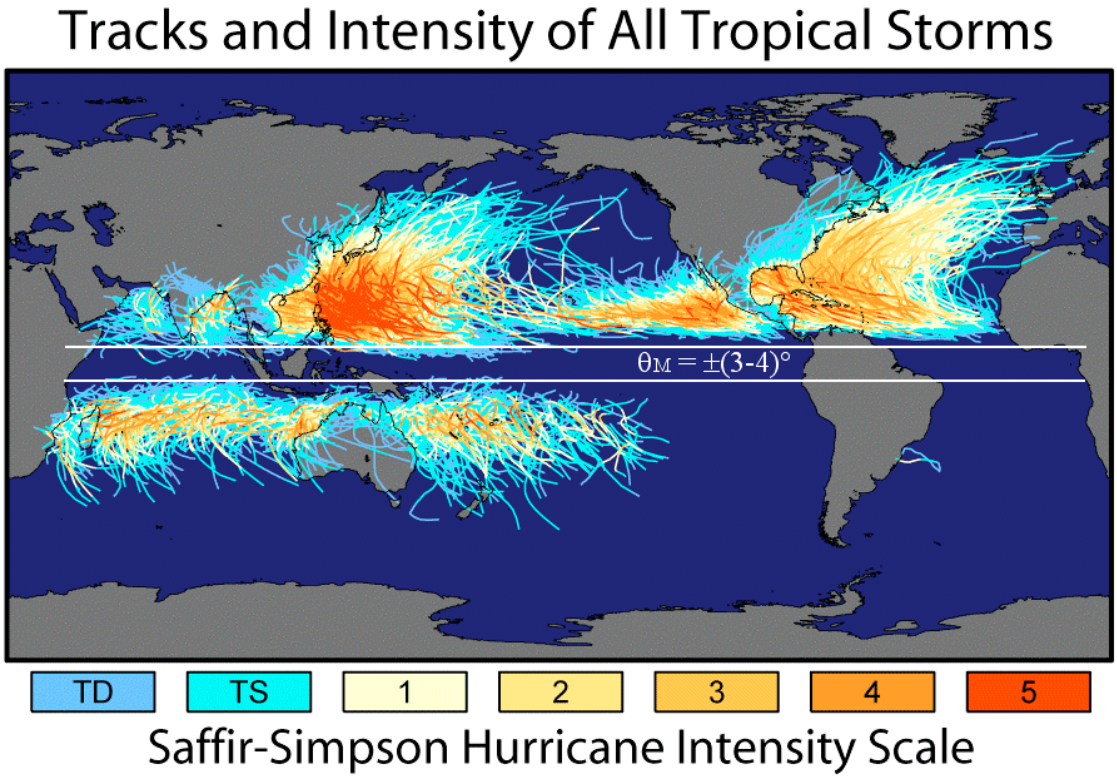

Figure 2 | Tropical storm tracks (1850-present). The tracks of tropical storms are shown in this figure color coded (from blue: tropical depression and tropical storm, to red: class 5 hurricane). The storms originate at the equator, fueled by hot tropical waters underneath a low-pressure region, and move towards the poles. In contrast to quantized vortices, the Earth's atmospheric vortices are classical objects that dissipate energy, especially when over colder waters, and they do not reach the poles. Tracking data for storms in the North Atlantic and East Pacific are from the National Hurricane Center. Tracking data for storms in the Indian Ocean, the Northwest and South Pacific are from the Joint Typhoon Warning Center. Tracking data for Hurricane Catarina in the South Atlantic was published in Gary Padgett's April 2004 Monthly Tropical Cyclone Summary. (Image courtesy of R.A. Rohde, available under a creative commons licence at http://www.globalwarmingart.com/). In the intensity scale, 'TD' means Tropical Depression, 'TS' is Tropical Storm, and the numbers refer to category 1-5 hurricanes or cyclones.

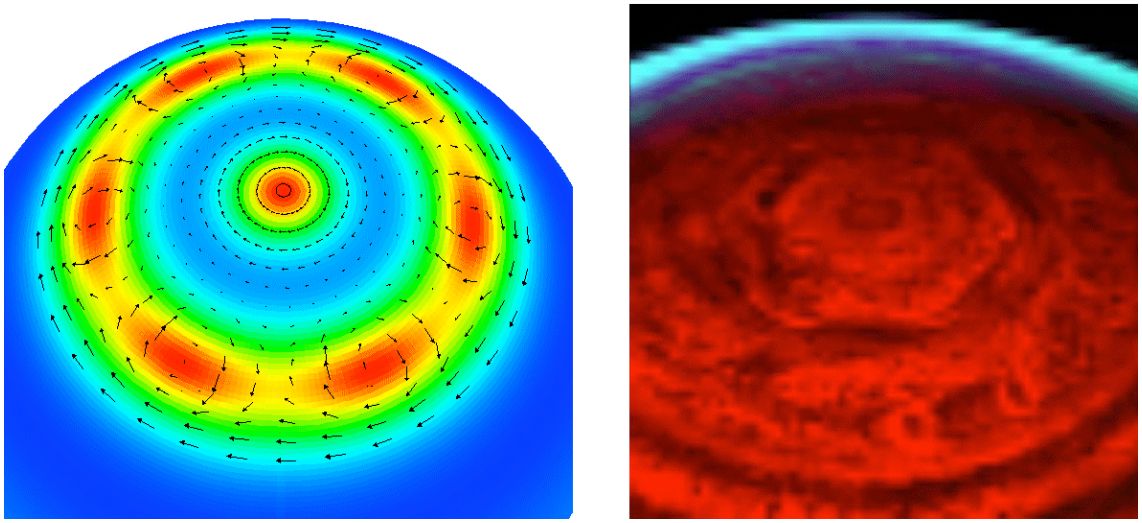

Figure 3 | Saturn's hexagon as a vortex lattice? This figure shows on the left a vortex pattern that arises at high magnetic field (H = 20) when a region of uniform vorticity breaks up into separate vortices. The color scale indicates the Cooper pair density, from blue (high) to red (low). The supercurrents are indicated by the arrow field. On the right, a cloud pattern observed at the north pole of Saturn (Credit: NASA/JPL/University of Arizona). Differential wind speeds (or superconducting currents) in two bands circling the pole leads to a depression (of pressure in the atmosphere, and of Cooper pair density in the superconductor) in the interface between the bands. A modulation of this depression reduces the energy in the case of a superconductor – one can speculate that a similar mechanism may be at work at Saturns pole. The initial state for the numerical calculations on the superconducting shell included nonuniform vorticity with a different angular momentum state near the poles and near the equator. The interface between the two regions with differential rotation splits up in individual vortices forming a vortex lattice similar to those obtained by ramping up the magnetic field and starting from a Meissner state. In both cases, the Meissner state co-exists with a vortex lattice at the poles.

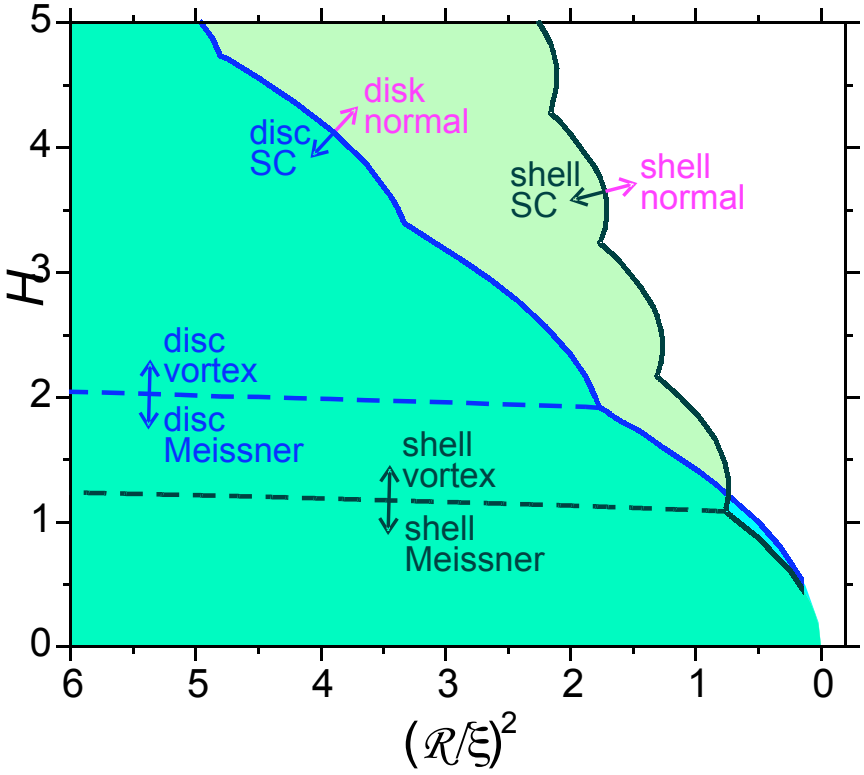

Figure 4 | **The phase diagram for a thin spherical shell** is compared to that of a flat disk. The shaded regions show the values of magnetic field and radius where the superconducting state is supported. The solid dark-green (blue) line corresponds to the boundary between the thermodynamically stable normal and superconducting states in shells (disks). The dashed dark-green (blue) line corresponds to the boundary between the thermodynamically stable Meissner and vortex states in shells (disks). The region in the phase diagram where vortex superconductivity is present is larger for shells than for disks. De Gennes showed that connecting a vorticity free region to a vorticity carrying region enhances superconductivity [8]. In nanoshells, this is realized by the coexistence of the vortex-free Meissner belt at the shell's equator with vorticity at the poles. This coexistence, absent in thin films, is enabled by the spherical topology of the shell.

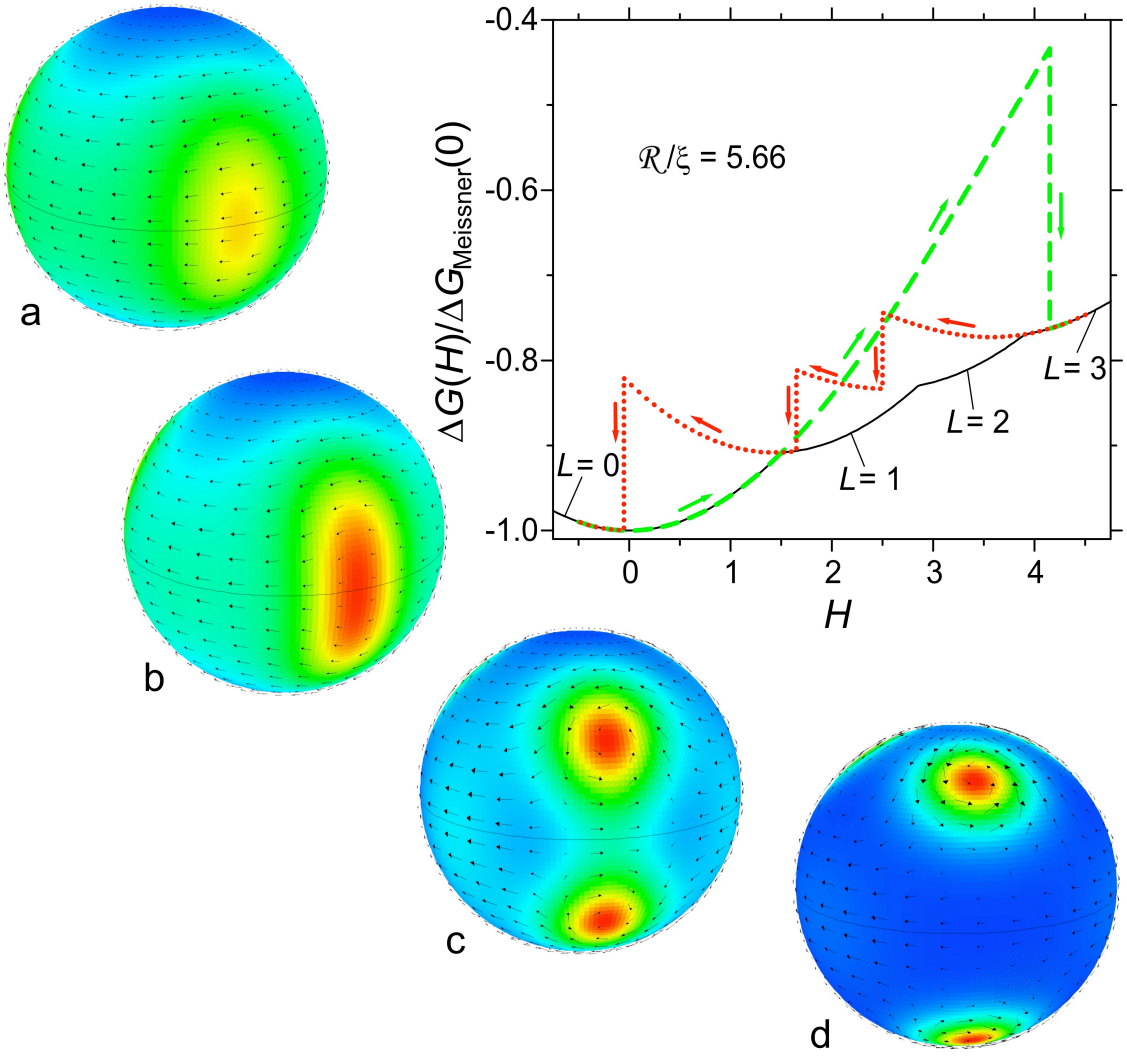

Figure 5 | Flux hysteresis in a superconducting nanoshell. The Gibbs free energy difference between the normal and superconducting state is plotted as a function of the magnetic field (expressed in number of elementary flux quanta through the equator), for a nanoshell with radius $\mathcal{R}/\xi$ = 5.66. The black curve shows the thermodynamically stable state. Below $H \approx 1.5$ the Meissner state (with L=0) prevails. For $1.5 < H < 2.85$, the state with a single vortex is stable. When the field is increased above $H = 2.85$ (3.9), the state with a second (third) vortex is thermodynamically stable. However, when the magnetic field is ramped up (green dashed curved), and down again (red dotted curve) a clear

hysteresis effect in the vorticity is seen. Indeed, when the field is slowly ramped up from 0 to 4.15, the vortex line is prohibited from entering the nanoshell: to enter the shell it has to nucleate at the shell's equator before it can migrate to the poles where it is thermodynamically stable. The energy necessary for nucleating vortices at the equator is reached at $H \approx 4.15$ when the shell makes a transition from the Meissner state to the state with three circulation quanta. Four snap shots of the dynamical process where vorticity enters the superconducting nanoshell are shown (a-d). The color scale indicates the Cooper pair density, from blue (high) to red (low). The supercurrents are indicated by the arrow field. A redistribution of the Cooper pair density is already present in the Meissner state (a). The vortices nucleate at a depression of the Cooper pair density at the equator (b), separate into two counterrotating two-dimensional vortices (c) and proceed towards the poles (d). There, they do not merge into a giant vortex, but rather remain at an equilibrium distance from each other and from the pole. When the magnetic field is then ramped down again, states with $L > 0$ persist metastably well below $H = 1.5$. To remove flux completely from this system, an external magnetic field has to be applied in the opposite direction ($H \approx -0.05$). The results depicted in this figure originate from a finite-element numerical solution of the time-dependent Ginzburg-Landau equation.